ARTICLE

Check for updates

Anomalous formation of trihydrogen cations from water on nanoparticles

M. Said Alghabra[1], Rami Ali[1,2], Vyacheslav Kim[1], Mazhar Iqbal[1], Philipp Rosenberger [3,4], Sambit Mitra[3,4], Ritika Dagar[3,4], Philipp Rupp[3], Boris Bergues[3,4], Deepak Mathur[5], Matthias F. Kling [3,4] & Ali S. Alnaser [1✉]

Regarded as the most important ion in interstellar chemistry, the trihydrogen cation, H_3^+, plays a vital role in the formation of water and many complex organic molecules believed to be responsible for life in our universe. Apart from traditional plasma discharges, recent laboratory studies have focused on forming the trihydrogen cation from large organic molecules during their interactions with intense radiation and charged particles. In contrast, we present results on forming H_3^+ from bimolecular reactions that involve only an inorganic molecule, namely water, without the presence of any organic molecules to facilitate its formation. This generation of H_3^+ is enabled by "engineering" a suitable reaction environment comprising water-covered silica nanoparticles exposed to intense, femtosecond laser pulses. Similar, naturally-occurring, environments might exist in astrophysical settings where hydrated nanometer-sized dust particles are impacted by cosmic rays of charged particles or solar wind ions. Our results are a clear manifestation of how aerosolized nanoparticles in intense femtosecond laser fields can serve as a catalysts that enable exotic molecular entities to be produced via non-traditional routes.

[1] Department of Physics, American University of Sharjah, Sharjah, UAE. [2] Department of Physics, The University of Jordan, Amman, Jordan. [3] Department of Physics, Ludwig-Maximilians-Universität Munich, Garching, Germany. [4] Max Planck Institute of Quantum Optics, Garching, Germany. [5] Department of Atomic and Molecular Physics, Manipal Academy of Higher Education, Manipal, India. ✉email: aalnaser@aus.edu

The trihydrogen cation, H_3^+, the simplest and most abundant triatomic ion in the universe, has continued to attract the research interest of numerous scientific communities since its discovery by J. J. Thomson in the early twentieth century[1]. Acting as a catalyst, H_3^+ is known to drive interstellar chemical reactions that lead to the creation of dense molecular clouds comprising diverse organic molecules[2,3]. As it behaves like a Brønsted–Lowry acid[4], the trihydrogen cation protonates interstellar ions, atoms, and molecules acting as the critically important precursor in the formation of complex organic compounds, which are believed to play a vital role in the creation of life in the universe[5,6]. It is not surprising then that the processes involved in the creation of H_3^+ have been the focus of many scientific investigations. Experiments investigating the formation of H_3^+ from organic compounds using electron impact[7,8], highly charged ion (HCI) collisions[9,10], and intense laser fields[11–15] are well documented in the literature. In these studies, usually a single organic molecule undergoes bond cleavage and bond formation in a two-step chemical process resulting in the creation of the trihydrogen cation. The first step involves a doubly charged precursor ion that breaks into a neutral H_2 molecule and a doubly charged fragment of the original organic molecule. In the second step of the mechanism, the roaming hydrogen molecule abstracts a proton from the doubly charged fragment, leading to the creation of an H_3^+ ion. At variance with all previous studies, in this work, we investigate the formation of the trihydrogen cation from inorganic molecules in a bimolecular mechanism encompassing two H_2O molecules adsorbed on the surfaces of silica nanoparticles in an intense femtosecond laser field.

As a hybrid between the atomic and the macroscopic realms, nanoparticles, and in general nanomaterials, are of increasing utility due to their unique characteristics and potential advantages in many science and engineering fields. For instance, nanoparticles have been utilized in laser acceleration of ions[16,17] and plasma dynamics[18]. In addition, based on their surface chemistry, nanoparticles have been shown to induce unexpected effects on biological tissues and cells. To illustrate, mesoporous silica nanoparticles have shown a remarkable ability as drug delivery agents when used in targeted cancer therapies, opening possibilities of a potentially safer and more effective treatment compared to contemporary methods such as chemotherapy[19]. The promising applications of nanoparticles in various fields are driving the extensive research on nanoscale materials. Specifically, in the light–matter interaction domain, intense femtosecond lasers have been used to study the effects of composition, shape, orientation, and size of nanostructures on their light absorption properties, and the spatial distribution of their photoion[20–22] and photoelectron[23–25] emissions in isolated nanoparticles and their clusters[26]. To further the understanding of the impact of the nanostructures' near-field on emitted photoions, Hickstein et al.[20] demonstrated how the composition of the nanostructures influence the momenta distributions of emitted photoions. Antonsson et al.[21] investigated the emission asymmetry of photoions ejected from NaCl nanoparticles as functions of size and laser intensity. On the other hand, Rupp et al.[22] demonstrated the enhancement in energy and momenta of protons dissociated from molecules inhabiting the surfaces of nanoparticles. Rosenberger et al.[26] highlighted the contrast in the momenta distribution of protons emitted from single nanoparticles compared to dimers. The aforementioned investigations have provided significant insights into the role of near-field enhancement in the photoion and photoelectron emissions from nanoparticles in intense laser fields[22–26]. However, in previous investigations[22,26], the parent atom or molecule of the emitted ions remained unconfirmed. Filling this lacuna would allow tracking and potentially controlling the molecular dynamics that lead to the generation of emitted

ions or electrons and assist in the development of new theoretical models. Here we present results that unravel complex and unique molecular dynamics carried by water/heavy water molecules adsorbed on the surfaces of SiO_2 nanoparticles to form H_3^+/D_3^+ ions. This bimolecular photochemical reaction, which involves proton/deuteron migration as well as bond cleavage and bond formation, is shown to lead to the formation of H_3^+/D_3^+ from two water/heavy water molecules. Our results offer unambiguous demonstration of yet another characteristic of nanoparticles as catalysts for exotic chemical reactions in intense femtosecond laser fields.

Results

In the present experiments, we employed the reaction nanoscopy technique[22], which enables measuring the three-dimensional momenta and energy of photoions. This experimental technique allows for differentiating between the charged fragments emitted from the nanoparticle surfaces and those generated from background gas constituents. To discriminate the ionization events associated with nanoparticles, where the electron emission signal is much higher compared to the signal from background gas constituents, we used a channeltron electron multiplier to record electron emission in coincidence with the ion emission. Further specifications of the experimental apparatus are schematically illustrated in the "Methods" section. We used a high-power, infrared fiber-based laser system (Active Fiber, central wavelength of 1030 nm) with a repetition rate of 150 kHz, pulse duration of ~40 fs, linearly polarized pulses, and focused intensities in the range of 1×10^{14} to 9.5×10^{14} W/cm^2.

To investigate the formation of H_3^+/D_3^+ from water/heavy water molecules adsorbed on the surface of silica nanoparticles, we conducted a series of experiments on SiO_2 nanoparticles (300 and 100 nm diameters), which were suspended in deionized H_2O and D_2O, prior to their injection into the vacuum chamber. The silica nanoparticles were exposed to laser intensities that are well-below the intensities where metallization is expected to occur and, therefore, the effects of plasmon excitations can be neglected in our current studies[27]. To ensure the accuracy of our experimental results, we confirmed, by Fourier-transform infrared (FTIR) spectroscopy, that our nanoparticles possessed a pure surface, devoid of any hydrocarbons; the surface exclusively comprised silanols (cf. Supplementary Fig. 1 showing FTIR spectra of the nanoparticles used in our experiments). The absence of hydrocarbons from the surfaces of nanoparticles is essential for our experiments, as it allows to precisely and unambiguously identify the source of the emitted trihydrogen and trideuterium ions.

Figure 1a shows typical time-of-flight (TOF) spectra of ions emitted from the surfaces of nanoparticles. Identifying the origin of the aforementioned ions was enabled by using the reaction nanoscopy method detailed in the "Methods" section. The TOF measurements show the formation of H_3^+ in addition to H^+ and H_2^+ ions. In addition, Fig. 1a shows that the formation of H_3^+ ions is nanoparticle-size independent. Although our TOF spectrometry succeeds in confirming the creation of the trihydrogen cation from water molecules adsorbed on the nanoparticle surfaces, the exact source of H_3^+ remains ambiguous as the silica nanoparticles' surfaces used in our experiments are inhabited by silanol groups in addition to water. As such, the production of H_3^+ may be a result of either water, silanol, or both. Therefore, to unambiguously identify the source of H_3^+ cations, we performed a different set of measurements with parameters identical to those mentioned above but using an isotopolog of water, namely D_2O. Substituting hydrogen by its isotope is a critical step in the process of identifying the exact origin of the trihydrogen cations, as the existence of deuterium is constrained to the heavy water molecules adsorbed on the nanoparticles' surfaces and cannot be
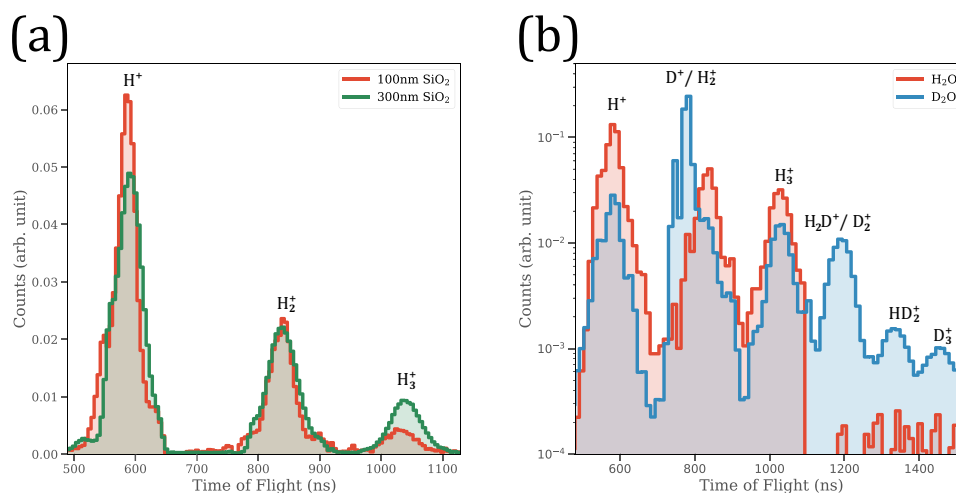
Fig. 1 Emitted ions from the surfaces of nanoparticles. a Comparison between two TOF spectra from two experiments (red/green lines) with different conditions including size of nanoparticles (100 and 300 nm), concentration of sample (3 and 1.5 g/L), and laser intensity at 2×10^{14} W/cm^2 serving as an evidence for the formation of H_3^+. **b** Comparison between ions emitted from the surfaces of 100 nm silica nanoparticles inhabited by H_2O and D_2O molecules at 3 g/L concentration and irradiated by a laser intensity of 2×10^{14} W/cm^2. The presence of D_3^+ and HD_2^+ peaks in the ToF spectrum of D_2O adsorbed on nanoparticles presents unequivocal evidence about the source of the trideuterium ions (for extended TOF spectra, cf. Supplementary Fig. 4). Source data are provided as a Source Data file.

found in silanol or any other constituents in our vacuum chamber. Figure 1b shows a comparison between the TOF spectra of 100 nm silica nanoparticles suspended in D_2O and H_2O. The observation of D_3^+ when D_2O is used as a suspension solution is unequivocal evidence in support of the formation from water adsorbed on the nanoparticle surface. Moreover, the existence of HD_2^+ in the TOF spectrum provides further confirmation, as it can only be produced when a D_2 moiety is formed through a migration mechanism in a single D_2O molecule followed by the abstraction of a proton from a neighboring silanol ion.

The TOF spectra in Fig. 1b reveal a considerable difference in yield between H_3^+ and D_3^+ emitted from the surfaces of nanospheres inhabited by H_2O and D_2O, respectively. The relative yield of the trihydrogen ion, which is calculated as the ratio of the area under the H_3^+ peak to the sum of areas under H^+, H_2^+, and H_3^+ peaks, was found to be 5.4% when produced from nanoparticle surfaces inhabited by H_2O. In the case of D_2O, we found the relative yield of D_3^+ emitted from D_2O molecules on the surface of silica nanoparticles to be ~0.38%. We have also measured the relative yield of HD_2^+ to be ~0.54%. Thus, the sum of the yields of D_3^+ and HD_2^+ remains less than that of H_3^+ emitted from the surface of silica nanospheres inhabited by H_2O. As isotopologs, H_2O and D_2O have nearly identical values of ionization energy[28] and a very similar intensity requirement to initiate the hydrogen migration process as well[29,30]. It is therefore expected that the relative yields of H_3^+ and D_3^+ will be similar. However, the difference in the yields between H_3^+ and D_3^+ suggests tantalizing possibilities of the existence of multiple novel pathways to form the trihydrogen cation as follows: (i) the production of H_3^+ exclusively from water adsorbed on the surface (ii) or solely from silanol, (iii) a hybrid process involving silanol and water wherein H_2 is formed from silanol, followed by acquisition of a proton from water, and (iv) a hybrid process where the H_2 is generated from water, which then abstracts a proton from silanol. If there were a significant exchange between D_2O and SiOH to generate deuterated silanols, D_3^+ would have been formed through four different pathways (similar to H_3^+ in the case of H_2O described above) and, consequently, the TOF spectra in Fig. 1b would have displayed a higher yield of D_3^+ compared to H_3^+ in the "D_2O on SiO_2" experiments, as, in this case, the formation of D_3^+ would have a pathway from deuterated silanol in addition to two

hybrid pathways and one solely from D_2O. However, based on our FTIR spectra taken at different time intervals of the particles in D_2O solution (cf. Supplementary Fig. 2) and the observed TOF spectra, we do not find any evidence suggesting significant deuteration of silanols under our experimental conditions.

The unimolecular migration process leading to the creation of H_2^+ and HD^+ ions from H_2O[30] and HOD[29] molecules, respectively, in an intense irradiating field has been documented before. According to Mathur et al.[29], producing the dihydrogen cation requires the application of few-cycle pulses (~7 fs) and laser intensity of ~1×10^{15} W/cm^2. Hence, we conducted a series of experiments on D_2O in the gas phase, to investigate the possibility of forming of D_2^+ ions at intensities, where both D_2^+ and D_3^+ are generated from D_2O molecules on the surfaces of nanoparticles. The TOF spectra from the experiments with gaseous D_2O are displayed in Fig. 2a. The results of our measurements did not yield any evidence for the creation of D_2^+ cations from D_2O in the gas phase, even at the highest intensity of ~1×10^{15} W/cm^2. At the same time, an incident intensity of 1×10^{14} W/cm^2, an order of magnitude lower, was sufficient to produce D_2^+ and D_3^+ cations from D_2O adsorbed on 100 nm SiO_2 particles (cf. Fig. 2b).

Based on the experimental evidence, we can conclude that silica nanoparticles act as a catalyst facilitating the formation of the trihydrogen/trideuterium cation from two water/heavy water molecules residing on the surface of the nanoparticles in a bimolecular photoreaction.

In addition to playing a catalyst role in forming H_3^+ and D_3^+ cations from water, we have discovered that the nanoparticles also facilitate the enhancement of momenta and energy of H_3^+/D_3^+ fragments formed on the surface of the nanoparticles. The enhancement is attributed to the formation of the near-field around the nanoparticle due to the interaction with a strong laser field, which is in accordance with earlier reports[22,26] on the enhancement of energy and momenta for protons dissociating from the surface of silica nanoparticles. Figure 3 shows the momenta and energy distributions of H_3^+ cations. The H_3^+ kinetic energy was found to have a mean value ~15 eV confirming the double role of nanoparticles as a facilitator of a bimolecular reaction between two water molecules and a source of enhancement in energy as well. Similarly, the mean energy for D_3^+ cations was also found to be ~15 eV (cf. Supplementary Fig. 7b).
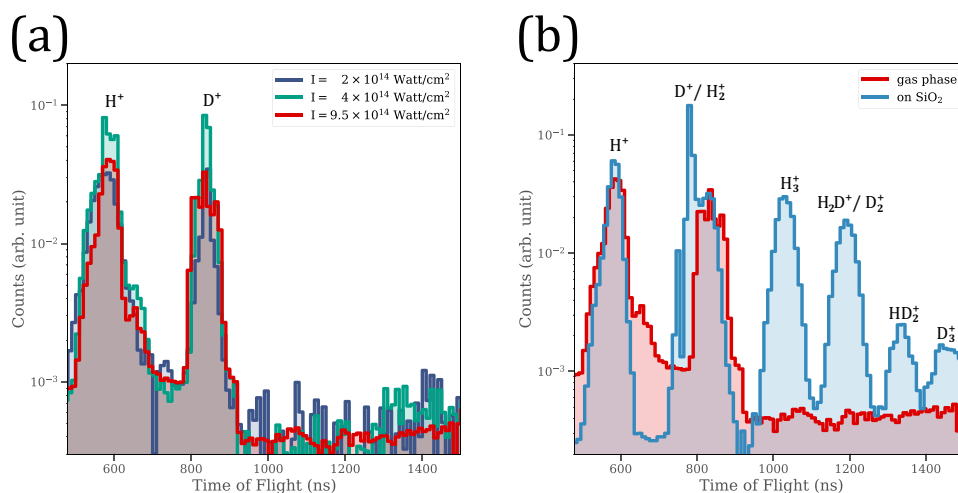
Fig. 2 Ion emission from D$_2$O in gas phase and on nanoparticles. a Comparison between time-of-flight spectra for D$_2$O in the gas phase for different laser intensities as indicated. The observed H$^+$ ions originate from background gas. **b** Comparison between TOF spectra taken for D$_2$O in the gas phase at 9.5 × 10^{14} W/cm^2 laser intensity and ions emitted from the surface of 100 nm nanoparticles inhabited by D$_2$O molecules at a laser intensity of 1 × 10^{14} W/cm^2. Only the spectrum associated with nanoparticles demonstrates the formation of D$_2^+$, HD$_2^+$, and D$_3^+$ ions. Source data are provided as a Source Data file.
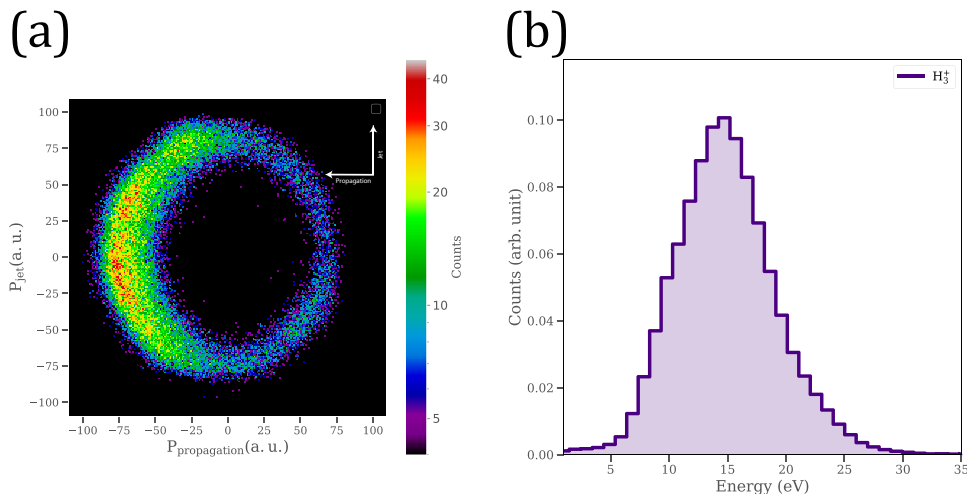

Fig. 3 Momentum and energy of H$_3^+$. a 2D momentum image demonstrating the angular distribution in the plane of laser propagation vs. nanoparticles jet where the laser polarization is perpendicular to this plane and **b** energy distribution of H$_3^+$ emitted from the surface of 300 nm silica nanoparticles inhabited by H$_2$O molecules at a laser intensity of 2 × 10^{14} W/cm^2. Source data are provided as a Source Data file.

Simulating the enhanced field around single silica nanoparticles[22] and their dimers[26] demonstrated how, for isolated nanoparticles, the near-field reaches its maximum intensity at the polar regions of the nanoparticle along the laser polarization, whereas in the case of a dimer, the near-field reaches its highest magnitude along the propagation direction. The angular distributions of H$_3^+$ (cf. Fig. 3a) and D$_3^+$ (cf. Supplementary Fig. 7a) show that the tri-hydrogen/trideuterium cations formed from water and heavy water, respectively, are mainly emitted from the surfaces of nanoparticles along the laser propagation direction. Such angular distribution is similar to what was previously observed with H$^+$ emitted from 300 nm silica nanoparticle clusters[26].

Discussion
Quantitative explanation of the processes involved in the formation of the high energy H$_3^+$ and D$_3^+$ ions observed in our experiments defies existing theoretical models. Any theoretical model that is to be developed needs to properly account for the dynamics of laser-field-induced ionization and fragmentation of water molecules on the surface of nanoparticles. In the absence of

such viable theoretical approaches, we take recourse to a qualitative rationalization of our experimental observations by postulating two potential mechanisms that could account for the creation H$_3^+$/D$_3^+$ from water molecules. These mechanisms are illustrated in Fig. 4. The first formation pathway (cf. green dashed line in Fig. 4) involves the aggregation of water molecules on the surface of SiO$_2$ nanoparticles. It is well known that each H-atom in a water molecule can be weakly attracted to a neighboring O-atom in an adjacent water molecule, leading to the formation of a hydrogen bond. Despite the relatively low energy of the hydrogen bond, estimated at ~250 meV[31], it is still sufficient to form a water dimer that is not destroyed by intramolecular thermal collisions at temperatures lower than 25 °C. The formation of such water clusters is not observed in our gas-phase experiments where our gas flow into the laser interaction zone is subsonic. Therefore, these aggregates must be a consequence of the nanoscale environment provided by the nanoparticles themselves. The creation of H$_3^+$/D$_3^+$ from water aggregates follows a two-step process involving both hydrogen/deuterium migration and roaming. In the first step, a migration process is initiated by the laser field
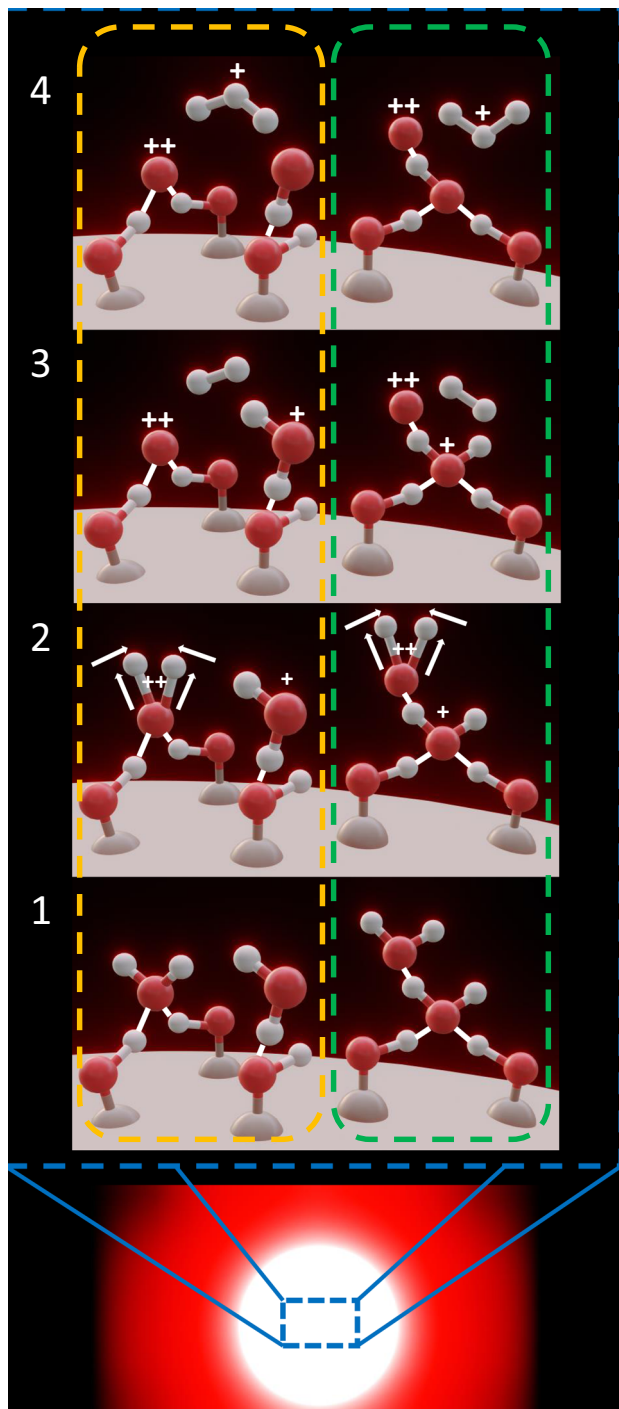
Fig. 4 Bimolecular reaction to form H_3^+ from water molecules on SiO_2 nanoparticles. An illustration of two potential processes responsible from the formation of H_3^+ from water molecules on the surface of silica nanoparticles. The bottom panel demonstrates a nanoparticle in an intense laser field. The orange dashed line depicts the formation of H_3^+ from two separate water molecules through a roaming on the surface mechanism. The green dashed line depicts the roaming mechanism within a water dimer. In both cases, there exist four stages. Stage 1 shows the ground state. Stage 2 shows the migration mechanism leading to the formation of a hydrogen molecule. Stage 3 is roaming close to another water ion. Stage 4 is the formation of H_3^+.

where the distance between the two hydrogen atoms decreases until a neutral H_2/D_2 moiety is dissociated from a doubly charged H_2O^{2+}/D_2O^{2+} ion. Second, the newly created hydrogen molecule abstracts a proton from its neighboring water ions as it roams around the water cluster, leading to the creation of an H_3^+/D_3^+ cation. The second plausible explanation for the H_3^+/D_3^+ production mechanism (orange dashed line in Fig. 4) is similar to what has already been observed and rationalized in unimolecular reactions in alcohol molecules[11–15]. The formation mechanism, similar to the process in clusters, involves both hydrogen migration and roaming. The migration step of the process remains unaffected; however, the roaming part of the procedure is altered in that the freshly produced H_2/D_2 molecule does not roam around its water cluster. Instead, the hydrogen molecule roams around the nanoparticle's surface, under the influence of the nanosphere's local field, and abstracts a proton from a neighboring water ion, thereby forming H_3^+/D_3^+ in a bimolecular reaction in contrast to a unimolecular reaction in alcohol molecules.

It is well established that when exposed to an intense electromagnetic field, nanoparticles experience an enhanced near-field with a spatial distribution that is different from the incident external beam[20–26]. Furthermore, the local field created around the nanoparticle has a higher intensity compared to the irradiating pulses. This enhancement in intensity differs depending on the nanoparticle's composition[20]. Simulating the field enhancement of SiO_2 nanoparticles using the finite-difference time-domain method yields a maximal intensity enhancement of 2.34 and 2.69 for isolated 100 and 300 nm particles, respectively[22], and 6.76 for dimers[26]. Still, the enhanced intensity obtained by using nanoparticles remains lower than the lowest intensity required to induce a migration mechanism in H_2O molecules in the gas phase according to Rajgara et al.[30], which is in accordance with our findings from the gas-phase experiments (cf. Fig. 2). The lower external intensity in our studies is not only adequate for initiating migration within a water molecule but also sufficient to start the complex mechanisms involved in forming the trihydrogen/trideuterium cations from two water/heavy water molecules on the surface of irradiated nanoparticles. Therefore, nanoparticles act as catalysts in the creation of H_3^+/D_3^+ by providing a unique nanoscale environment. This nanoscale environment encompasses the near-field intensity enhancement, as well as the trapped electrons[25] and local charges interactions, which can facilitate the opening of such a novel reaction.

To summarize, we have conducted a series of experiments involving intense laser irradiation of water and heavy water molecules adsorbed on the surfaces of silica nanoparticles. Our findings offer unambiguous evidence of SiO_2 nanoparticles playing the role of catalysts in the formation of H_3^+/D_3^+ with high kinetic energy and surprisingly high yields. The creation of H_3^+/D_3^+ requires, of necessity, a bimolecular reaction between two water molecules on the surface of nanoparticles. We have demonstrated the possibility of probing complex molecular reactions occurring on the surface of nanoparticles in an intense laser field. These results should reinvigorate efforts to overcome the profound theoretical challenges that are currently faced in developing proper theoretical insights into molecular dynamics that occur concomitantly in intense optical fields and on the surfaces of nanostructures. There is growing contemporary evidence that the implications of such dynamics may well extend beyond the domain of the chemical sciences and into the biological sciences[32]. In the context of the fact that the existence of H_n^+ entities in diverse astrophysical environments has been conjectured for about six decades[33], the experimental results that

5

we present here may be relevant to astrophysics and astro-chemical environments, and in particular to the evolving field of dust astronomy. Although the environment conducive to the production of trihydrogen cation presented in this work was engineered in our terrestrial laboratory, nature has engineered its own parallel environment. It is now well established that dust in both the inner heliosphere and planetary debris discs around other stars does include nanometer-sized dust particles ranging in size from a few tens to a few hundreds of nanometers[34,35]. Indications of hydrated cometary interplanetary dust particles followed by laboratory studies suggest that hydrated silicates may form in the near-surface regions of comets if liquid water is present[36]. It is not unrealistic, then, to expect these dust nano-particles to act as catalysts for the formation of trihydrogen cation, or other molecular species requiring similar conditions, if these nanoparticles are impacted by cosmic rays of charged particles or solar wind HCIs.

To further elaborate on this point, it has been established that in collisions with charged particles, molecular targets experience fields equivalent to half-cycle pulses, "virtual photons," of similar magnitudes to those of intense fields of femtosecond, or shorter, laser pulses of several optical cycles[9,37]. The time-dependent effective intensity $I_{eff}(t)$ depends on the impact parameter, charge state, and velocity of the charged particle with peak intensities that can easily exceed 10^{13} W/cm^2. In addition, the experimental observation of the formation of H_3^+ cations in low energy (1.2 MeV $\approx$ 2400 km/s) collisions of Ar^{8+} ions with gas-phase methanol led to the suggestion that collisions of HCI with organic molecules is a possible mechanism for the formation of H_3^+ in space[9]. Following Bhardwaj et al.[37], the effective peak intensity for the 2400 km/s Ar^{8+} ions at an impact parameter of 3 Å would be $\sim$3.5$\times$10^{13} W/cm^2, whereas the effective peak intensity for a fast ($\approx$800 km/s) solar wind HCI of similar charge state such as Ne^{8+}, Mg^{8+}, Si^{8+}, or Fe^{8+} ions would be $\sim$1.2$\times$10^{13} W/cm^2, which is about one-third that of the Ar^{8+} laboratory effective peak intensity. Given that the present results have demonstrated that for D$_2$O adsorbed on SiO$_2$ nanoparticles, the production of D$_2^+$ and D$_3^+$ cations required an incident femtosecond laser intensity one order of magnitude lower than

that needed to produce D$_2^+$ cations from D$_2$O in the gas phase, hydrated dust nanoparticles in space may indeed act as catalysts for the formation of H$_3^+$ cations under the impact of solar wind HCI of somewhat smaller effective peak intensities than that of Ar^{8+}. Cosmic rays of charged particles, on the other hand, can give rise to effective peak intensities several orders of magnitude larger than those of solar wind HCI at sub-attosecond timescales and may readily initiate the sequence of events leading to the formation of H$_3^+$ from hydrated dust nanoparticles. In this con-text, the historical connection between attosecond atomic colli-sions and ultrashort light pulses has been recently summarized in ref. [38].

Methods

Experimental setup. To conduct the experiments, we employed the reaction nanoscope technique[22] illustrated in Fig. 5. We used a high-power fiber-based laser system (Active Fiber) at a central wavelength of 1030 nm, repetition rate of 150 kHz, pulse durations of around 40 fs, linearly polarized pulses along the electric field, and intensities in the range of 1×10^{14} to 9.5×10^{14} W/cm^2. The laser was tightly focused inside the reaction nanoscope's ultrahigh vacuum chamber using a spherical silver back-focusing mirror. We used two sets of silica nanospheres with a diameter of 300 and 100 nm as targets. To ensure the accuracy of our experimental results, we used nanoparticles with a pure surface, such that it is clean from any hydrocarbons and is inhabited by silanol (SiOH) exclusively. The absence of hydrocarbons from the surfaces of nanoparticles is essential for our experiments, as it allows us to precisely identify the source of the emitted H$_3^+$/D$_3^+$ ions. These nanoparticles were suspended and sonicated in deionized H$_2$O/D$_2$O and the mixture was aerosolized using a constant output atomizer (TSI 3076). The aerosol is delivered into the ultrahigh vacuum chamber through an aerodynamic lens, creating a jet of aerosolized nanoparticles crossing the laser beam path, at the center of the chamber, resulting in the formation of ion fragments from the H$_2$O/D$_2$O molecules that were adsorbed by the silanol groups on the surface of the nanoparticles. The reaction nanoscopy technique permits three-dimensional momentum imaging of charged fragments, from which their kinetic energies can be obtained. In the experiments, we measure the TOF and the impact position of ions using a delay-line detector equipped with two microchannel plates and a delay-line anode.

Ions origin identification. To distinguish ions emitted from the surface of the nanoparticles from those originating in the background gas in the chamber, we utilized a channeltron electron multiplier (Photonis Magnum). The channeltron records the number of electrons associated with each laser shot. Nanoparticles generate a larger number of photoelectrons when interacting with the laser pulses compared to the background gas. This in turn allows the identification of ions
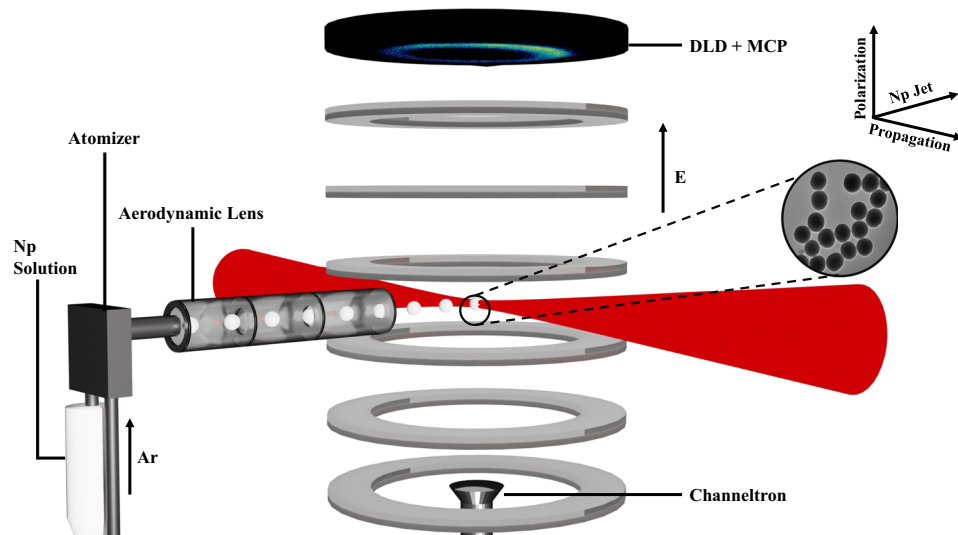

Fig. 5 Experimental setup. Illustration of the experimental setup showing the nanoparticle solution (Np Solution) that is aerosolized by an atomizer with the help of Ar as carrier gas. The aerosol is then collimated using the aerodynamic lens producing a jet that is admitted to the ultrahigh vacuum chamber. The nanoparticles interact with the laser field in the center of a constant-field (E) spectrometer. The ions generated from the interaction are accelerated towards a microchannel plate (MCP) and delay-line detector (DLD). As for the electrons, they are accelerated towards a channeltron and are used to discriminate between nanoparticles and background ions. The inset shows a scanning electron microscope (SEM) image of the silica nanoparticles (NanoComposix) used in the experiments.
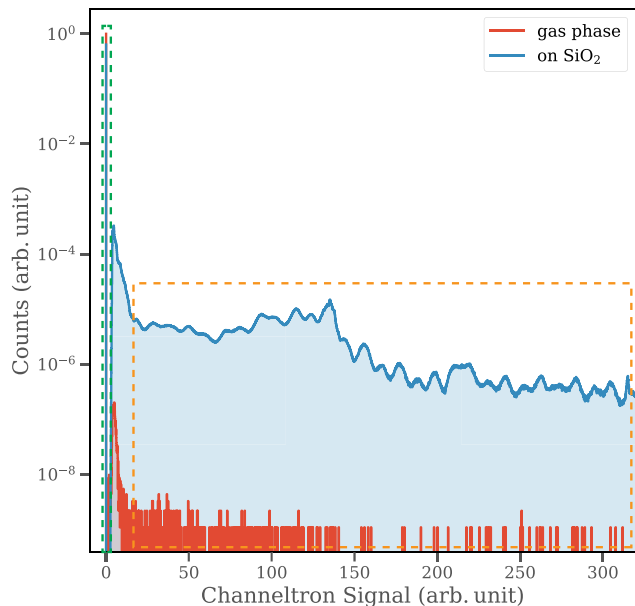
Fig. 6 Channeltron signal for gas-phase and nanoparticle targets. Figure 6 displays accumulated distributions from ~1 billion pulses in the experiment. A considerable difference in channeltron signal between gas phase and nanoparticles D_2O targets. The red line represents the channeltron signal for D_2O in the gas phase, whereas the blue curve demonstrates the signal associated with nanoparticles. Both measurements were performed at a laser intensity of 2×10^{14} W/cm^2. The vast majority of laser shots result in no channeltron signal as indicated by the black dashed line. The orange dashed line highlights how laser shots associated with irradiating nanoparticles generate a significantly larger channeltron signal, which in turn is used in coincidence with the time-of-flight spectra to extract the time of flight for ions associated with nanoparticles. Source data are provided as a Source Data file.

associated with nanoparticles only by filtering the TOF signal measured in coincidence with a high channeltron signal. Figure 6 demonstrates the considerable difference in channeltron signal between nanoparticles and the background gas constituents.

Data availability

The data that support the findings of this study are available from the corresponding author (A.S.A.) upon reasonable request. Source data are provided with this paper.

References

1. Thomson, J. J. XXVI. Rays of positive electricity. *Philos. Mag. J. Sci.* **21**, 225–249 (1911).
2. Smith, D. The ion chemistry of interstellar clouds. *Chem. Rev.* **92**, 1473–1485 (1992).
3. Smith, D. & Španěl, P. Dissociative recombination of H_3^+ and some other interstellar ions: a controversy resolved. *Int. J. Mass Spectrom. Ion. Process.* **129**, 163–182 (1993).
4. Lowry, T. The uniqueness of hydrogen. *J. Soc. Chem. Ind.* **42**, 43–47 (1923).
5. Watson, W. D. Interstellar molecule reactions. *Rev. Mod. Phys.* **48**, 513 (1976).
6. Dalgarno, A. & Black, J. Molecule formation in the interstellar gas. *Rep. Prog. Phys.* **39**, 573 (1976).
7. Kushawaha, R. & Bapat, B. Fragmentation dynamics of the methanol dication. *Chem. Phys. Lett.* **463**, 42–46 (2008).
8. Burrows, M., Ryan, S., Lamb, W. Jr & McIntyre, L. Jr Studies of H^+, H^+, and H^+ dissociative ionization fragments from methane, ethane, methanol, ethanol, and some deuterated methanols using electron-impact excitation and a time-of-flight method incorporating mass analysis. *J. Chem. Phys.* **71**, 4931–4940 (1979).
9. De, S., Rajput, J., Roy, A., Ghosh, P. & Safvan, C. Formation of H_3^+ due to intramolecular bond rearrangement in doubly charged methanol. *Phys. Rev. Lett.* **97**, 213201 (2006).
10. De, S., Roy, A., Rajput, J., Ghosh, P. & Safvan, C. Dissociation of methanol by ion-impact: Breakup dynamics, bond rearrangement and kinetic energy release. *Int. J. Mass Spectrom.* **276**, 43–48 (2008).
11. Furukawa, Y., Hoshina, K., Yamanouchi, K. & Nakano, H. Ejection of triatomic hydrogen molecular ion from methanol in intense laser fields. *Chem. Phys. Lett.* **414**, 117–121 (2005).
12. Okino, T. et al. Coincidence momentum imaging of ejection of hydrogen molecular ions from methanol in intense laser fields. *Chem. Phys. Lett.* **419**, 223–227 (2006).
13. Okino, T. et al. Ejection dynamics of hydrogen molecular ions from methanol in intense laser fields. *J. Phys. B Atom. Mol. Opt. Phys.* **39**, S515 (2006).
14. Ekanayake, N. et al. Mechanisms and time-resolved dynamics for trihydrogen cation (H_3^+) formation from organic molecules in strong laser fields. *Sci. Rep.* **7**, 1–12 (2017).
15. Ekanayake, N. et al. H_2 roaming chemistry and the formation of H_3^+ from organic molecules in strong laser fields. *Nat. Commun.* **9**, 1–11 (2018).
16. Cho, M. H., Pathak, V. B., Kim, H. T. & Nam, C. H. Controlled electron injection facilitated by nanoparticles for laser wakefield acceleration. *Sci. Rep.* **8**, 1–8 (2018).
17. Ostermayr, T. M. et al. Proton acceleration by irradiation of isolated spheres with an intense laser pulse. *Phys. Rev. E* **94**, 033208 (2016).
18. Hickstein, D. D. et al. Observation and control of shock waves in individual nanoplasmas. *Phys. Rev. Lett.* **112**, 115004 (2014).
19. Mamaeva, V., Sahlgren, C. & Lindén, M. Mesoporous silica nanoparticles in medicine—recent advances. *Adv. Drug Deliv. Rev.* **65**, 689–702 (2013).
20. Hickstein, D. D. et al. Mapping nanoscale absorption of femtosecond laser pulses using plasma explosion imaging. *ACS Nano* **8**, 8810–8818 (2014).
21. Antonsson, E. et al. Size-dependent ion emission asymmetry of free NaCl nanoparticles excited by intense femtosecond laser pulses. *Phys. Chem. Chem. Phys.* **21**, 12130–12138 (2019).
22. Rupp, P. et al. Few-cycle laser driven reaction nanoscopy on aerosolized silica nanoparticles. *Nat. Commun.* **10**, 1–7 (2019).
23. Zherebtsov, S. et al. Controlled near-field enhanced electron acceleration from dielectric nanospheres with intense few-cycle laser fields. *Nat. Phys.* **7**, 656–662 (2011).
24. Zherebtsov, S. et al. Carrier–envelope phase-tagged imaging of the controlled electron acceleration from SiO_2 nanospheres in intense few-cycle laser fields. *N. J. Phys.* **14**, 075010 (2012).
25. Powell, J. A. et al. Interplay of pulse duration, peak intensity, and particle size in laser-driven electron emission from silica nanospheres. *Opt. Express* **27**, 27124–27135 (2019).
26. Rosenberger, P. et al. Near-field induced reaction yields from nanoparticle clusters. *ACS Photonics* **7**, 1885–1892 (2020).
27. Liu, Q. et al. Ionization-induced subcycle metallization of nanoparticles in few-cycle pulses. *ACS Photonics* **7**, 3207–3215 (2020).
28. Reutt, J., Wang, L., Lee, Y. & Shirley, D. Molecular beam photoelectron spectroscopy and femtosecond intramolecular dynamics of H_2O^+ and H_2O^+. *J. Chem. Phys.* **85**, 6928–6939 (1986).
29. Mathur, D., Dharmadhikari, A. K., Dharmadhikari, J. A. & Vasa, P. Hydrogen migration within a water molecule: formation of HD^+ upon irradiation of HOD with intense, ultrashort laser pulses. *J. Phys. B* **50**, 154004 (2017).
30. Rajgara, F., Dharmadhikari, A., Mathur, D. & Safvan, C. Strong fields induce ultrafast rearrangement of H atoms in H_2O. *J. Chem. Phys.* **130**, 231104 (2009).
31. Feyereisen, M. W., Feller, D. & Dixon, D. A. Hydrogen bond energy of the water dimer. *J. Phys. Chem.* **100**, 2993–2997 (1996).
32. Nayek, U. et al. Strong strand breaks in DNA induced by thermal energy particles and their electrostatic inhibition by Na+ nanostructures. *J. Phys. Chem. A* **123**, 3241–3247 (2019).
33. Mathur, D. & Hasted, J. B. Odd and even numbered hydrogen ion clusters. *Nature* **280**, 573–574 (1979).
34. Mann, I. Comets as a possible source of nanodust in the Solar System cloud and in planetary debris discs. *Philos. Trans. R. Soc. A Math. Phys. Eng. Sci.* **375**, 20160254 (2017).
35. Grün, E., Krüger, H. & Srama, R. The dawn of dust astronomy. *Space Sci. Rev.* **215**, 46 (2019).
36. Nakamura-Messenger, K., Clemett, S. J., Messenger, S. & Keller, L. P. Experimental aqueous alteration of cometary dust. *Meteorit. Planet. Sci.* **46**, 843–856 (2011).
37. Bhardwaj, V. R. et al. Dissociative ionization of gas-phase chloromethanes by intense fields of picosecond and attosecond duration. *Phys. Rev. A* **58**, 3849 (1998).
38. Burgdörfer, J., Lemell, L. & Tong, X.-M. 60 years of attosecond physics at ICPEAC: from collisions to ultrashort pulses. *J. Phys. Conf. Ser.* **1412**, 022001 (2020).

Author contributions

A.S.A. conceived and supervised the study. M.S.A. and R.A. prepared and performed the experiments. M.S.A. analyzed the data. A.S.A. and M.F.K. introduced the nanoTRIMS concept. M.S.A., R.A., P. Rupp, P. Rosenberger, S.M., and R.D. set up the experimental apparatus. V.K. and M.I. provided the laser beam and assisted in performing the measurements. Final interpretations were carried out by M.S.A., R.A., A.S.A., M.F.K., P. Rosenberger, and B.B. with contributions from other authors. Many valuable insights and suggestions were provided by D.M. All authors discussed the results and contributed to the final manuscript drafted by M.S.A. and A.S.A.

Competing interests

The authors declare no competing interests.

Additional information

Supplementary information The online version contains supplementary material available at https://doi.org/10.1038/s41467-021-24175-9.

Correspondence and requests for materials should be addressed to A.S.A.

Peer review information *Nature Communications* thanks Marcos Dantus, Daniel Slaughter, and the other, anonymous, reviewer for their contribution to the peer review of this work. Peer reviewer reports are available.

Reprints and permission information is available at http://www.nature.com/reprints

Publisher's note Springer Nature remains neutral with regard to jurisdictional claims in published maps and institutional affiliations.